Effective pairing interaction induced by polarization effects in deformed nuclei

2005 J. Phys. G: Nucl. Part. Phys. 31 295

(http://iopscience.iop.org/0954-3899/31/5/002)

INSTITUTE OF PHYSICS PUBLISHING JOURNAL OF PHYSICS G: NUCLEAR AND PARTICLE PHYSICS

J. Phys. G: Nucl. Part. Phys. **31** (2005) 295–307 doi:10.1088/0954-3899/31/5/002

Effective pairing interaction induced by polarization effects in deformed nuclei

P Donati[1,2], G Gori[1,2], F Barranco[3], R A Broglia[1,2,4] and E Vigezzi[2]

[1] Dipartimento di Fisica, Università degli Studi di Milano, via Celoria 16, 20133 Milano, Italy
[2] INFN, Sezione di Milano, via Celoria 16, 20133 Milano, Italy
[3] Departamento de Fisica Aplicada III, Universidad de Sevilla, Escuela Superior de Ingenieros, Camino de los Descubrimientos s/n, 41092 Sevilla, Spain
[4] Niels Bohr Institute, University of Copenhagen, Blegdamsvej 17, 2100 Copenhagen Ø, Denmark

Received 4 January 2005
Published 22 February 2005
Online at stacks.iop.org/JPhysG/31/295

Abstract
The effective pairing interaction induced by the exchange of phonons between pairs of nucleons moving in time-reversal states close to the Fermi energy in deformed nuclei modifies in a sizeable manner the superfluid properties of these systems, accounting for about half of the pairing gap.

Communicated by Professor A Covello

1. Introduction

Many properties of atomic nuclei are strongly influenced by the tendency nucleons have to form Cooper pairs, eventually leading to the phenomenon of nuclear superfluidity. In particular, superfluidity in deformed nuclei modifies in an important way the moment of inertia of these systems, being also responsible for the backbending phenomenon (nuclear quake) in which the Coriolis force, acting as an external magnetic field, breaks Cooper pairs, eventually inducing a phase transition (superfluid-normal) strongly renormalized by quantal-size effects (cf, e.g., [1, 2] and references therein).

It has been shown in the case of spherical nuclei that an important contribution to the formation of the pairing condensate arises from the renormalization of the nucleon–nucleon interaction due to the dynamical polarization of the nuclear medium [3–6]. The origin of this effective interaction is connected with the exchange of low-lying collective surface vibrations among nucleons moving in time-reversal states close to the Fermi energy. The nuclear surface, generated by the self-consistent motion of nucleons, is not only a static barrier confining the motion of the nucleons but it also renormalizes the single-particle properties in processes where nucleons, bouncing inelastically off the surface, sets it into vibration (cf figure 1). These vibrational modes can, at a later time, be reabsorbed by the same nucleon (effective mass processes) or by a different nucleon leading to an effective interaction (cf figure 2 (b)).

The role the particle-vibration coupling has on the effective mass and on the associated level density around the Fermi energy in deformed, rapidly rotating nuclei, has been studied

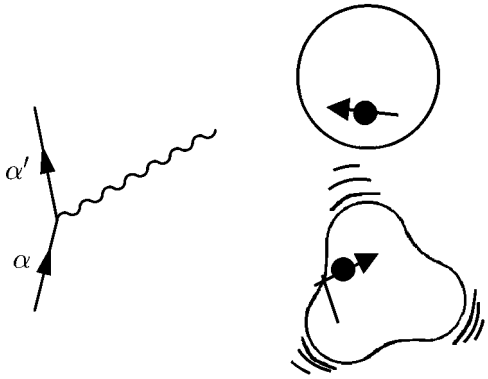

Figure 1. On the left, the diagram describing the particle vibration coupling [9], while on the right the schematic representation of a nucleon scattering inelastically off the nuclear surface producing the emission of a phonon.

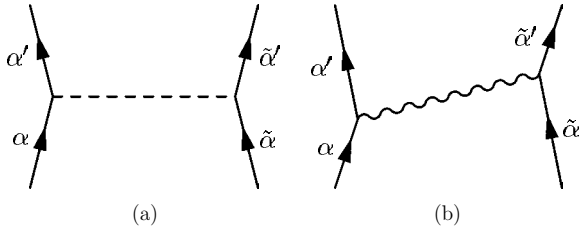

Figure 2. Scattering process induced by the pairing force associated with the Hamiltonian defined in equation (1). Single-particle states are represented by arrowed lines and labelled by the quantum number α. The state $|\tilde{\alpha}\rangle$ is obtained from the state $|\alpha\rangle$ by the operation of time reversal. (a) Bare pairing interaction (dashed horizontal line) of strength G_0 (cf equation (5)). (b) Induced pairing interaction arising from the exchange of vibrations (represented by a wavy line) between pairs of nucleons moving in time-reversal states $|\alpha\tilde{\alpha}\rangle$, $|\alpha'\tilde{\alpha}'\rangle$ lying close to the Fermi energy.

in [7]. It was found that coupling effects renormalize the nucleon mass to a value that is 40% larger than that of the bare nucleon mass. This result is found to be about 50% smaller than that obtained in the case of the spherical nuclei [8]. This is a consequence of the surface rigidity of deformed nuclei as compared to spherical nuclei, surface rigidity associated with the fact that most of the quadrupole collectivity of surface degrees of freedom is absorbed into the static deformation of the mean field.

Motivated by these results and by those of [3], we have studied the contribution of core polarization to pairing correlations in superfluid deformed nuclei. Our work should be considered as a first step, towards a more comprehensive study that should include self-energy renormalization and vertex corrections in the same theoretical framework, as was recently done in the case of the superfluid, spherical nucleus ^{120}Sn [6]. On the other hand, at least in spherical nuclei, the pairing gap resulting from this more general approach turns out to be rather similar to that obtained considering only the exchange of collective vibrations.

2. Formalism

The single-particle states used in the calculations are determined making use of a mean field potential (Nilsson potential). In the associated particle-hole basis, the excited states of the

deformed nuclei were calculated within the framework of the quasi-particle random phase approximation (QRPA). We then calculate the induced interaction between pairs of nucleons moving in time-reversal states arising from the exchange of these vibrational modes. Making use of the resulting pairing interaction

$$H = -\sum_{\alpha,\alpha'>0} G_{\alpha\alpha'} a^{\dagger}_{\alpha} a^{\dagger}_{\tilde{\alpha}} a_{\tilde{\alpha}'} a_{\alpha'}, \tag{1}$$

the state-dependent BCS pairing gap

$$\Delta_{\alpha} = \sum_{\alpha'>0} G_{\alpha\alpha'} \frac{\Delta_{\alpha'}}{2E_{\alpha}} \tag{2}$$

is determined with the condition

$$N = 2\sum_{\alpha>0} V_{\alpha}^2. \tag{3}$$

In the above expression

$$E_{\alpha} = \sqrt{\left(\epsilon_{\alpha} - G_{\alpha\alpha} V_{\alpha}^2 - \lambda\right)^2 + \Delta_{\alpha}^2} \tag{4}$$

is the quasi-particle energy associated with the single-particle state with quantum number α, while

$$G_{\alpha\alpha'} = G_0 + G^{\mathrm{ind}}_{\alpha,\alpha'}, \tag{5}$$

is the sum of the bare pairing interaction (cf figure 2(a))

$$G_0 = \frac{C}{A}\ \mathrm{MeV} \tag{6}$$

and of the induced pairing interaction $G^{\mathrm{ind}}_{\alpha\alpha'}$ (cf figure 2(b)) arising from the exchange of phonons (nuclear vibrations). The constant C in equation (6) will be adjusted so as to reproduce the experimental findings, as explained below. Note that we neglect the contribution of the phonons (i.e. neglecting $G^{\mathrm{ind}}_{\alpha\alpha'}$), $G \approx 25/A$ MeV. In order to calculate the quantity $G^{\mathrm{ind}}_{\alpha\alpha'}$, use is made of the nuclear field theory (cf, e.g., [9] and references therein) describing the structure of the atomic nucleus in terms of single-particle and collective vibrations and their coupling, as well as the four-point vertices of the nucleon–nucleon bare interaction. The Hamiltonian describing these degrees of freedom and their coupling can be written as

$$H = \hat{h}_{\mathrm{def}} + \sum_{nLK} \hbar\omega_n(LK)\left(\hat{\Gamma}^{\dagger}_n(LK)\hat{\Gamma}_n(LK) + \frac{1}{2}\right) + \hat{H}_c \tag{7}$$

where $\hat{h}_{\mathrm{def}}$ is the Nilsson Hamiltonian while $\Gamma^{\dagger}_n(LK)$ is an operator which creates a phonon with energy $\hbar\omega_n(LK)$. The L and K quantum numbers indicates that phonons are the solution of QRPA equations associated with a residual multipole–multipole interaction

$$\hat{H}_{LK} = \frac{1}{2}\chi_{LK}\hat{Q}^{\dagger}_{LK}\hat{Q}_{LK}, \qquad \hat{Q}_{LK} = \sum_{a=1}^{A}(r^L Y_{LK})_a \tag{8}$$

where the spherical harmonic functions Y_{LK} are defined with respect to the symmetry axis z (cf [10] and references therein). We shall only consider the quadrupole ($L = 2$) and octupole ($L = 3$) terms. In order to include the effect of deformation, use has been made of the doubly stretched [11] coordinates to write the multipole operators.

$\hat{H}_c$ in equation (7) is the term that couples the fermionic degrees of freedom to the bosonic degrees of freedom, which we write as

$$\hat{H}_c = -\sum_{LK} \chi_{LK}\hat{\alpha}_{LK}\hat{F}_{LK},$$

where

$$\hat{\alpha}_{LK} = \sum_n z_n(LK)\big(\hat{\Gamma}^\dagger_n(LK) + (-1)^{L-K}\hat{\Gamma}_n(L-K)\big).$$

The quantity $z_n(LK) = (\hbar\omega_n(LK)/2C_n(LK))^{1/2}$ is the zero-point fluctuation associated with the phonon state $|nLK\rangle \equiv \Gamma^\dagger_n(LK)|0\rangle$. It is obtained from the QRPA calculation of the vibrational modes through the relation

$$z_n(LK) = \langle 0|\big[\hat{F}_{LK}, \Gamma^\dagger_n(LK)\big]_{RPA}|0\rangle = \sum_{ij} M_{ij}(LK)(X_n(ij;LK) + Y_n(ij;LK)), \tag{9}$$

where $\hat{F}$ is the single-particle operator acting on the fermionic degrees of freedom

$$\hat{F}_{LK} = \sum_{ij} M_{ij}(LK)\big[A^\dagger_{ij}(LK) + (-1)^{L-K}A_{ij}(L-K)\big],$$

with

$$A^\dagger_{ij}(LK) = \big[a^\dagger_i, a_j\big]_{LK},$$

and

$$M_{ij}(LK) = \langle i|r^L Y_{LK}|j\rangle,$$

while the *RPA* phonon operator is

$$\Gamma^\dagger_n(LK) = \sum_{ij,n}\big[X_n(ij,LK)A^\dagger_{ij}(LK) + (-)^{L-K}Y_n(ij,LK)A_{ij}(L-kK)\big]$$

and the quantities $X_n(ij,LK)$ and $Y_n(ij,LK)$ are the forward and backward *RPA* amplitudes renormalized according to

$$\sum_{ij}\big[X^2_n(ij,LK) - Y^2_n(ij,LK)\big] = 1.$$

The coupling constants χ_{LK} are adjusted in order to reproduce within the framework of the QRPA, the energy and the transition probability of the low-lying states. The induced pairing interaction associated with the exchange of vibrations between time-reversal single-particle states can then be written as

$$G^{\rm ind}_{\alpha\alpha'} = 2\times\sum_{nLK}\chi^2_{LK}z^2_n(LK)\frac{\langle\alpha|\hat{F}^*_{LK}|\alpha'\rangle\langle\bar{\alpha}|\hat{F}_{LK}|\bar{\alpha}'\rangle}{E_0 - (|\epsilon_\alpha-\lambda| + |\epsilon_{\alpha'}-\lambda| + \hbar\omega_n(LK))}$$
$$-2\times\sum_{nLK}\chi^2_{LK}z^2_n(LK)\frac{\langle\alpha|\hat{F}^*_{LK}|\bar{\alpha}'\rangle\langle\bar{\alpha}|\hat{F}_{LK}|\alpha'\rangle}{E_0 - (|\epsilon_\alpha-\lambda| + |\epsilon_{\alpha'}-\lambda| + \hbar\omega_n(LK))}. \tag{10}$$

The minus sign associated with the second term is connected with the antisymmetrization of the wavefunctions while the factor 2 which multiplies both terms is connected with the two possible time orderings of the process shown in figure 2(b).

The quantity

$$E_0 = U - E_{\rm unp}, \tag{11}$$

is the pair correlation energy, the difference between the ground state energy including pairing correlations

$$U = \sum_{\alpha>0}(\epsilon_\alpha-\lambda)V^2_\alpha - \sum_{\alpha\alpha'>0}G_{\alpha\alpha'}\frac{\Delta_\alpha}{E_\alpha}\frac{\Delta_{\alpha'}}{E_{\alpha'}}, \tag{12}$$

and the unperturbed ground state energy

$$E_{\rm unp} = \sum_{\substack{\alpha>0 \\ (\epsilon_\alpha \leqslant \epsilon_F)}} (\epsilon_\alpha - \epsilon_F). \tag{13}$$

The set of equations (2), (3), (10) and (11) are to be solved simultaneously (Bloch–Horowitz approximation), and lead to a self-consistent value of Δ_α. Taking an average over levels close to the Fermi energy (within an energy interval $|\epsilon_\alpha - \lambda| \leqslant 2\Delta \approx 2$ MeV), one obtains an estimate of Δ which can be compared with the experimental values.

While the values of $G^{\rm ind}_{\alpha\alpha'}$ are fixed by the energies $\epsilon_\alpha, \hbar\omega_L(n)$, the particle-vibration coupling strengths $z_n(LK)$ and the single-particle matrix elements $\langle\alpha'|r^L Y_{LK}|\alpha\rangle$, one has to adjust C in equations (5) and (6) in order to reproduce the experimental findings. Calculations of the pairing gap as discussed above were performed for a series of isotopic chains, namely samarium, gadolinium, dysprosium and erbium. In the case of samarium isotopes, we have considered both spherical and deformed nuclei, while in the other cases only well-deformed nuclei have been included.

The empirical values for the pairing gap can be obtained making use of odd–even mass differences. An often employed formula is the three-point relation

$$\Delta_n(N, Z) = -\tfrac{1}{2}[B(N-1, Z) - 2B(N, Z) + B(N+1, Z)], \tag{14}$$

where $B(N, Z)$ is the binding energy [12] associated with the nucleus ${}^A_N X_Z$ of mass $A = N+Z$.

3. Results

We start by discussing the results obtained for ^{A}Sm-isotopes ($A = 146, 148, 150, 152, 154$). In this chain ^{146,148}Sm are spherical, while ^{152,154}Sm are well deformed and ^{150}Sm is a transitional nucleus.

The gap for these isotopes derived from the odd–even mass differences displays a rather characteristic bell-shape behaviour, as can be seen from figure 3 where the values of Δ_n calculated making use of equation (14) are displayed. Another source of information concerning the pairing gap is given by the two-particle transfer cross section. This is because

$$\begin{aligned}\sigma(t, p; gs(N) \to gs(N+2)) &\sim \left|\langle \mathrm{BCS}(N+2)| \sum_{\alpha>0} a^\dagger_\alpha a^\dagger_{\tilde\alpha} |\mathrm{BCS}(N)\rangle\right|^2 \\ &= \left(\sum_{\alpha>0} U_\alpha(N) V_\alpha(N+2)\right)^2, \end{aligned} \tag{15}$$

in keeping with the fact that to transfer two neutrons to the target nucleus with N neutrons the single-particle levels have to be empty, and this happens with amplitude $U_\alpha(N)$, while the same level in the residual (final nucleus) has to be filled, and this takes place with probability $V_\alpha(N+2)$.

Making use of the BCS relations

$$U_\alpha(N)V_\alpha(N) = \frac{\Delta(N)}{2E_\alpha(N)}, \qquad \sum_{\alpha>0} U_\alpha(N)V_\alpha(N) = \frac{\Delta(N)}{G(N)}, \tag{16}$$

it is seen that the ground state (t, p) cross section is intimately connected with the square of the pairing gap. In analogy with the three-points formula for Δ_n introduced in equation (14),

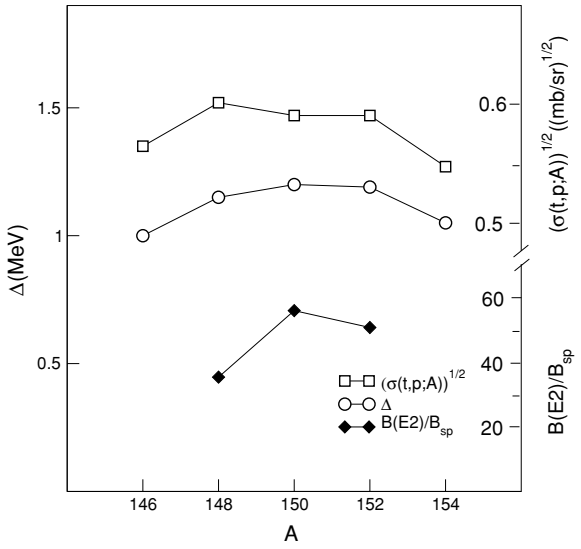

Figure 3. The neutron pairing gap of the ^{A}Sm isotopes obtained making use of mass data [12] and of equation (14), in comparison with the square root of the average value of the (t, p)-cross section derived from the experimental results reported in [13] (cf also [14]) and making use of equation (17). Also displayed are the summed values of the $B(E2)$ transition probability (in terms of single-particle units) connecting the low-energy 2^+ states with the ground state for the spherical nuclei ^{148}Sm and the transitional nucleus ^{150}Sm (we include the states lying at 551 keV (33 spu), 1453 keV (3 spu) ($A = 148$); 334 keV (55 spu), 1046 keV (1 spu) ($A = 150$)); as well as the β- and the γ-vibrations with the 0^+ and 2^+ members of the ground state rotational band in ^{152}Sm 685 keV (33 spu), 811 keV (1 spu and 5 spu), 1084 keV (3.4 spu and 9 spu)) [15].

we define

$$\overline{\sigma(t,\,p;\,A)} \sim \left(\frac{\Delta_n(A)}{G(A)}\right)^2$$
$$= \frac{1}{3}[\sigma(t,\,p;\,gs(A-2) \to gs(A) + \sigma(t,\,p;\,gs(A) \to gs(A+2)$$
$$+ \sigma(t,\,p;\,gs(A+2) \to gs(A+4)], \tag{17}$$

where $\sigma(t,\,p;\,gs(A) \to gs(A+2))$ stands for the ground state cross section measured at the first maximum. Making use of the differential cross section of [13], one obtains the results shown in figure 3, displaying a mass dependence which is in overall agreement with that shown by Δ_n (same figure). It is revealing that a similar behaviour is displayed by the square of the quadrupole deformation parameters β_2 (or by the electromagnetic transition probabilities, cf also figure 3), which is one of the main spectroscopic inputs needed to calculate the induced pairing interaction $G^{\rm ind}_{\alpha\alpha'}$ defined in equation (10).

We now proceed to calculate $G^{\rm ind}_{\alpha\alpha'}$. The basic elements needed to carry out this microscopic calculation are: the single-particle levels, the collective vibrations and the particle-vibration coupling vertices. In the case of the ^{146}Sm, ^{148}Sm (spherical) and ^{150}Sm (transitional) nuclei, the single-particle levels were calculated making use of a Saxon–Woods potential with standard parametrization [16]. The levels around the Fermi energy are shown in figure 4. For the deformed nuclei ^{152}Sm and ^{154}Sm, the single-particle levels are those associated with a deformed Nilsson potential [17] with the parameters proposed in [18]. The deformation parameters were fixed using a Nilsson–Strutinsky technique [19, 20]. In this basis the BCS

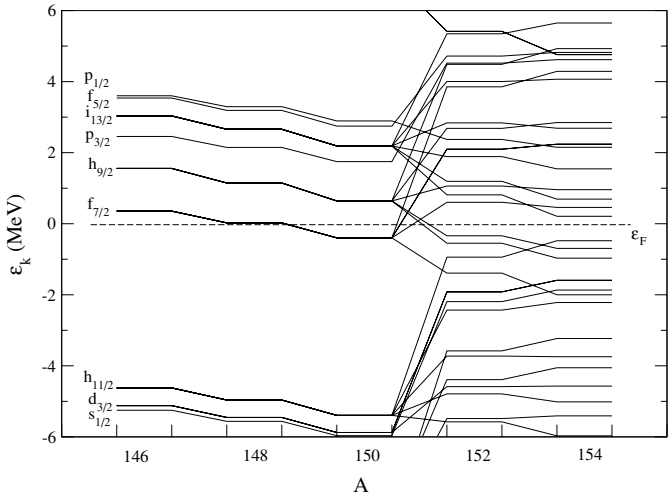

Figure 4. Single-particle levels around the Fermi energy used in the calculation of Sm-isotopes. For ^{146}Sm, ^{148}Sm, ^{150}Sm, the single-particle levels are those associated with a spherical Woods–Saxon potential with the parametrization taken from [16]. For the deformed nuclei ^{152}Sm, ^{154}Sm we have used the levels associated with the deformed Nilsson potential (see text). The energies are measured with respect to the Fermi ϵ_F energy calculated by solving the BCS equations.

solution was worked out with $G = 25/A$. The vibrational modes were calculated in the QRPA [10] in the corresponding two-quasi-particle basis by diagonalizing the separable multipole–multipole interaction introduced in equation (8). The corresponding strengths χ_{LK} were adjusted so as to best reproduce the energy and the transition probabilities of the different low-lying modes. In the case where these values were not known, the Sakamoto–Kishimoto prescription [11] was used.

Special attention was paid to the $L = 2$, $K = 1$ spurious state associated with the breaking of rotational invariance by the intrinsic state of deformed nuclei. In this case the coupling constant χ_{21} was tuned to obtain a QRPA solution at zero energy, which was then excluded in the calculation of interaction induced by exchange of phonons.

The different parameters entering the calculations and results obtained for 2^+ and 3^- excitations are collected in tables 1 and 2, respectively. It is found that the exchange of 2^+ phonons contributes 90% of the global interaction induced by medium polarization effects. One can understand the small contribution arising from the exchange of 3^- phonons by considering the sequence of levels of the neutron valence shell reported in figure 4. With the exception of the state $i_{13/2}$, there appear only single-particle levels with negative parity, which can therefore exchange only positive-parity phonons. On the other hand, the level $i_{13/2}$, due to the angular momentum conservation, can interact by the action of 3^- phonons only with the $h_{9/2}$ and to the $f_{7/2}$ levels; the coupling with the former level is moreover reduced due to the fact that it involves a flip of the single-particle spin.

In figure 5 we display the pairing matrix elements, arising from the exchange of β, γ and octupole vibrations (cf equation (10)) for the spherical nucleus ^{148}Sm and for the deformed nucleus ^{152}Sm. The value of $G^{\rm ind}_{\alpha\alpha'}$ is plotted as a function of the single-particle energies ϵ_α and $\epsilon_{\alpha'}$. Because of the energy denominator in equation (10), exchange of phonons induces large pairing matrix elements only between pairs of particles moving close to the Fermi energy. Therefore in figure 5 we show the matrix elements only for states which lie within

Table 1. The calculated energy and transition amplitude $\tau(E\lambda : I_i K_i \rightarrow 0) = \sqrt{B(E\lambda : I_i K_i \rightarrow 0)}$ of five samarium isotopes, compared with the experimental values for the lowest excited 2^+ states. The experimental data are from [21, 22]. We used the prescription discussed in [23] to derive the values of τ from the QRPA calculation. In the last column is listed the quantity $z_n(LK)$ (cf equation (9)) associated with the lowest excited 2^+ states. In the case of ^{150}Sm two calculations were performed, one using a spherical ground state (†) and one using a well-deformed ground state (*).

		Energy (MeV)		τ (fm^2)		$z_n(LK)$
Nucleus	Transition	Calculation	Experiment	Calculation	Experiment	(fm^2)
^{146}Sm	2^+	0.82	–	33.82	–	79.58
^{148}Sm	2^+	0.52	0.55	38.45	36.05	91.73
^{150}Sm†	2^+	0.32	0.33	48.81	50.79	118.00
^{150}Sm*	$2^+\beta$	1.13	1.05	17.9	6	61.7
	$2^+\gamma$	1.19	1.19	32.80	10.39	63.20
^{152}Sm	$2^+\beta$	0.924	0.81	14.45	6.78	56.24
	$2^+\gamma$	1.185	1.09	20.41	13.03	58.92
^{154}Sm	$2^+\beta$	1.18	1.18	11.56	11.74	49.63
	$2^+\gamma$	1.44	1.44	16.44	6.32	55.37

Table 2. The same as table 1, but for the lowest excited 3^- states.

		Energy (MeV)		τ (fm^3)		$z_n(LK)$
Nucleus	Transition	Calculation	Experiment	Calculation	Experiment	(fm^3)
^{146}Sm	3^-	1.385	–	234	–	552.2
^{148}Sm	3^-	1.401	1.162	226	224	540.4
^{150}Sm†	3^-	1.524	1.072	217	214	527.4
^{150}Sm*	$3^-\ K=0$	2.029	–	259	–	324.6
	$3^-\ K=1$	2.102	–	42	–	310.5
	$3^-\ K=2$	2.349	–	34	–	268.6
	$3^-\ K=3$	2.468	–	34	–	31.8
^{152}Sm	$3^-\ K=0$	0.940	1.041	139	131	664
	$3^-\ K=1$	1.560	1.578	100	100	212
	$3^-\ K=2$	1.878	–	55	–	409
	$3^-\ K=3$	2.241	–	8	–	18
^{154}Sm	$3^-\ K=0$	1.011	1.011	118	113	639
	$3^-\ K=1$	1.797	–	43	–	157
	$3^-\ K=2$	2.226	–	19	–	148
	$3^-\ K=3$	2.053	–	11	–	20

± 5 MeV around the Fermi energy. In order to distinguish the matrix elements associated with different m-projections in the spherical case, we have artificially split the degenerate single-particle levels associated with the spherical nucleus ^{148}Sm, plotting the modified single-particle energies

$$\epsilon^*_\alpha = \epsilon_\alpha + (0.2\ \text{MeV}) \times m_\alpha$$

where m_α is the angular momentum projection of the spherical state α.

In the spherical case, the vibrations couple more or less democratically to the single-particle states regardless of their angular momentum projection or, equivalently, regardless of the spatial orientation of the initial and final single-particle orbital. In the case of the deformed

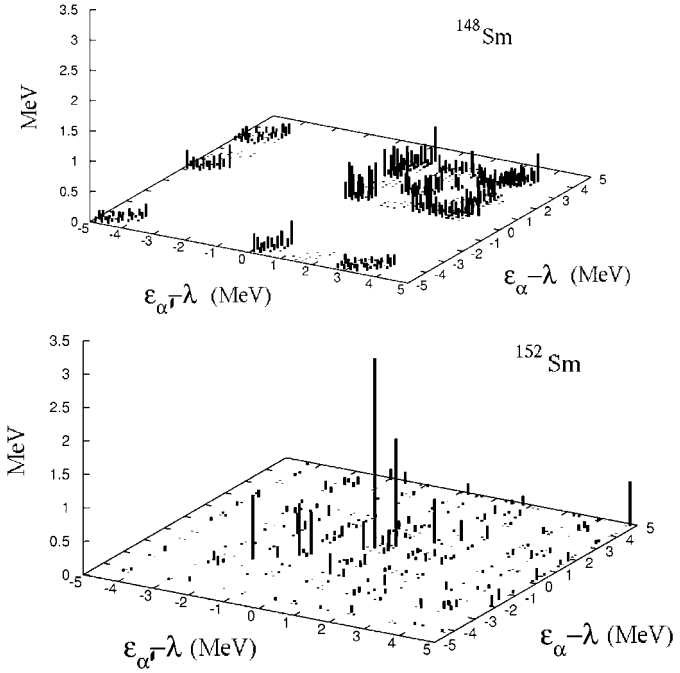

Figure 5. The induced pairing matrix elements $G^{\rm ind}_{\alpha\alpha'}$ (cf equation (10)) for the spherical nucleus ^{148}Sm and the deformed nucleus ^{152}Sm, plotted as a function of $\epsilon_\alpha - \lambda$ (x-axis) and $\epsilon_{\alpha'} - \lambda$ (y-axis), where λ is the Fermi energy.

nucleus, in contrast, one finds a small number of single-particle states whose diagonal matrix element is very large. One can check that these orbitals have large angular momentum and low projection along the symmetry axis. Their wavefunctions are thus strongly aligned (with the deformation of the system). β-vibrations are thus particularly effective to induce scattering processes between pairs of time-reversal orbits of this type.

The small number of sizeable off-diagonal matrix elements is of importance when we solve the BCS equations by considering only the scattering induced by exchange of phonons (cf figure 2(b)). As we can see from figure 6 (upper panel), these processes lead to a state-dependent pairing gap peaked at the Fermi surface for the spherical nucleus ^{148}Sm. In contrast to the deformed nucleus ^{152}Sm, the lack of a sufficient number of off-diagonal matrix elements results in the trivial solution for the BCS equation, i.e. $\Delta = 0$. The processes induced by exchange of phonons are not able, alone, to produce off-diagonal correlations strong enough to switch on the superfluid phase. In this respect, we observe that the BCS equations are usually solved neglecting the term $G_{\alpha\alpha}V_\alpha^2$ in equation (4), because its effect is a simple renormalization of the single-particle energies. However, in the present case, where the diagonal matrix elements are much larger than the level spacings, this term plays an important role and must be retained.

But this does not mean that we can neglect the induced interaction in the discussion of the nuclear pairing properties for deformed nuclei. In fact, besides the induced interaction, scattering between pairs of particles in time-reversal state is produced by the bare nucleon–nucleon potential. We mimic the effects of this bare potential by using a constant matrix element $G_0 = 16/A$ MeV ($\approx$0.11 MeV) instead of $G = 25/A$ MeV ($\approx$0.18 MeV) when the nucleons are scattered between states which lie 5 MeV within the Fermi energy. We chose

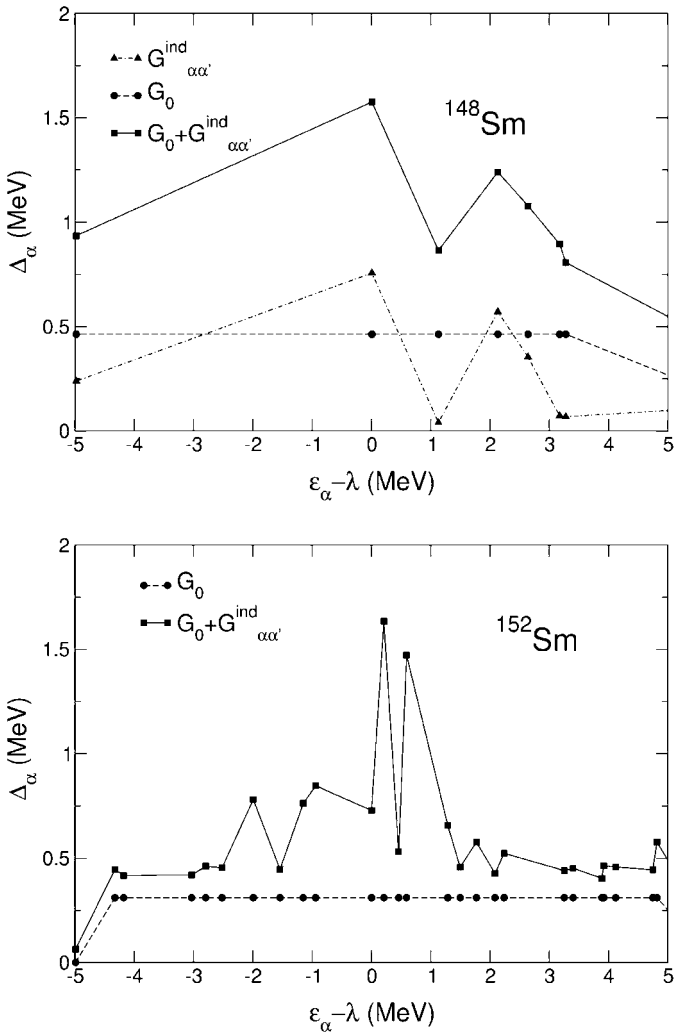

Figure 6. Pairing gap Δ_α, solution of the BCS equations, displayed as a function of the single-particle energy measured from the Fermi energy, for different choices of the pairing matrix elements: considering only the scattering produced by exchange of phonons (solid triangles), considering only the constant G_0 (solid dots), taking into account both these contributions (solid squares). Note that in the case of ^{152}Sm there is no solution (but the trivial $\Delta_\alpha = 0$) associated with the exchange of phonons alone (see discussion in the text).

this value of G_0 because, on the average, it allows us to reproduce the experimental value of the different nuclei we studied. We may appreciate the role of the induced interaction in the deformed nucleus ^{152}Sm by looking at the lower panel of figure 6. In this figure is shown the BCS pairing gap obtained by using $G_0 = 16/A$ MeV alone or by adding to it the induced pairing matrix elements $G^{\rm ind}_{\alpha\alpha'}$.

In figure 7 we compare our results with experimental data. In the lower panel we display the gap associated with the different Sm-isotopes obtained by averaging the corresponding values of Δ_α shown in figure 6, over an energy range of the order of twice the largest Δ_α value. In the case of ^{150}Sm two different calculations were performed, the first one where

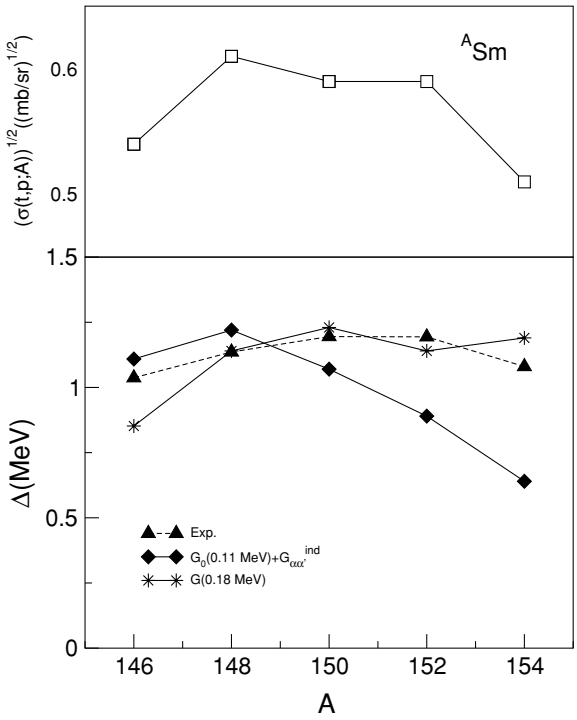

Figure 7. Upper panel: the square root of the average value of the t, p-cross section calculated making use of the results reported in [13] already shown in figure 3 (cf equation (17)). Lower panel: the empirical values of the pairing gap for the different Sm-isotopes, derived from equation (14), are compared with the theoretical results calculated by solving self-consistently equations (2), (3), (10) and (11) using $G_0 + G^{\rm ind}_{\alpha\alpha'}$ with $G_0 = 16/A$ MeV (≈ 0.11 MeV). Also shown are the gaps obtained with only the bare pairing interaction, with $G = 25/A$ MeV ($\approx$0.18 MeV).

the nucleus was assumed to be vibrational, and the second deformed. The large difference between the structure parameters obtained testifies to the fact that the QRPA is not applicable to the transitional nucleus ^{150}Sm, and that anharmonicity effects are likely to be very large. The value of Δ reported in figure 7 corresponds to the average between these two values. It is seen that the pairing gap obtained by adding the induced pairing interaction to the constant $G_0 = 0.11$ MeV accounts for the experimental value. As a rule, if one neglects the induced interaction contribution, a value of $G = 0.18$ MeV would be needed to obtain those averages.

In figure 8 we display the results of calculations carried out as discussed above for the case of a number of well-deformed Gd, Dy and Er isotopes. We have chosen these isotopes for convenience, because we can make use of the study presented in [23], where the deformation parameters and the experimental information available for these nuclei are reported together with the results of a QRPA calculation. We have used the same input data and reproduced their results concerning the energies and the strengths of phonons.

Concerning the effects of the interaction induced by the exchange of phonons on the pairing gap, we can draw similar conclusions as those obtained in the case of the deformed Sm-isotopes presented above. The main contributions to $G^{\rm ind}_{\alpha\alpha'}$ arise from coupling of single-particle motion to β- and γ-vibration, the contributions arising from octupole phonons being negligible. In all these lanthanide isotopes, the induced interaction is not able alone to switch on a

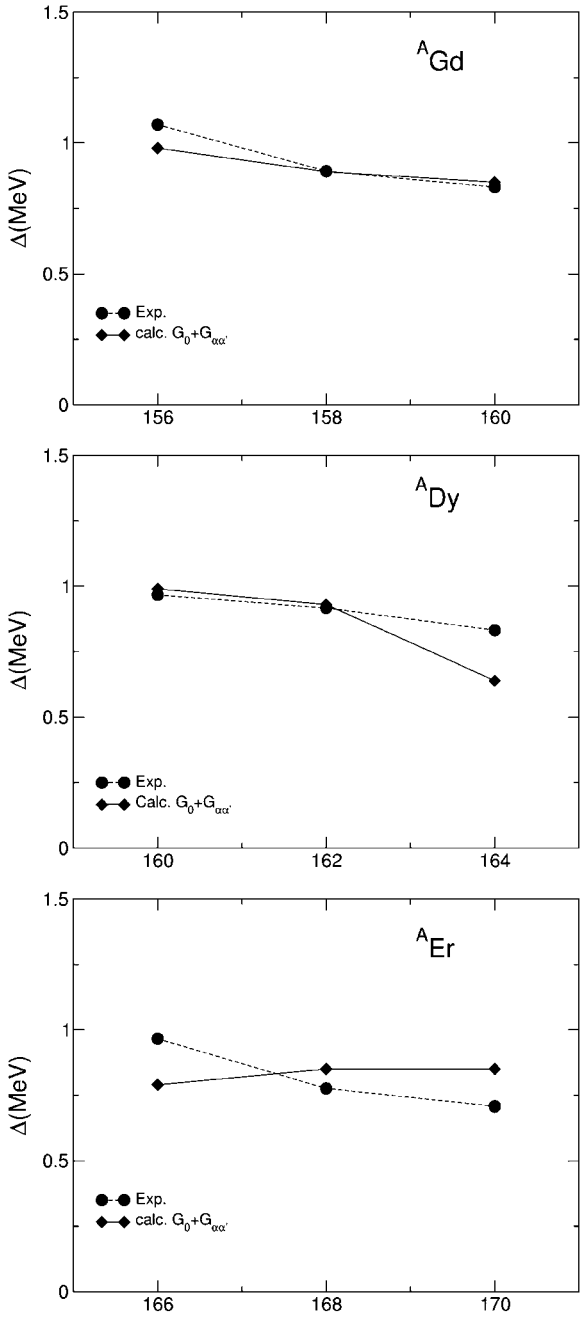

Figure 8. The empirical pairing gaps of a series of deformed Gd- (top), Dy- (middle) and Er-isotopes (bottom), derived from the experimental masses making use of relation (14), are compared with the theoretical values obtained by adding the induced interaction to a bare force with $G_0 = 0.11$ MeV.

superfluid phase. However, it gives an appreciable contribution to the pairing gap, once it is added to the bare nucleon–nucleon pairing force. In fact, one can reproduce the overall

empirical values of the pairing gap using a constant $G = 0.18$ MeV. This value is reduced to $G_0 = 0.11$ MeV, including the induced interaction matrix elements between states lying 5 MeV within the Fermi energy.

4. Conclusions

The induced pairing interaction arising from the exchange of β, γ and octupole phonons between pairs of single-particle states moving close to the Fermi energy accounts for ≈40% of the pairing gap, the rest arising from the bare nucleon–nucleon interaction which can be approximately described by a constant matrix element $G = 0.11$ MeV ($\approx 16/A$ MeV) between states which lie 5 MeV within the Fermi energy.

References

[1] Stephens F S 1975 *Rev. Mod. Phys.* **41** 43
[2] Brink D and Broglia R A 2005 *Nuclear Superfluidity: Pairing in Finite Systems* (Cambridge: Cambridge University Press) at press
[3] Barranco F *et al* 1999 *Phys. Rev. Lett.* **83** 2147
[4] Terasaki J *et al* 2002 *Nucl. Phys.* A **697** 127
[5] Terasaki J *et al* 2002 *Prog. Theor. Phys.* **108** 495
[6] Barranco F *et al* 2004 *Eur. Phys. J.* A **21** 57
[7] Donati P *et al* 2000 *Phys. Rev. Lett.* **84** 4317
[8] Mahaux C *et al* 1985 *Phys. Rep.* **120** 1
[9] Bortignon P F *et al* 1977 *Phys. Rep.* **30c** 305
[10] Donati P *et al* 1999 *Nucl. Phys.* A **653** 225
[11] Sakamoto H and Kishimoto T 1989 *Nucl. Phys.* A **501** 205
[12] Audi G and Wapstra A H 1995 *Nucl. Phys.* A **595** 409
[13] Bjerregaard J H, Hansen O and Nathan O 1966 *Nucl. Phys.* **86** 145
[14] Broglia R A *et al* 1973 *Adv. Nucl. Phys.* **6** 287
[15] Bohr A and Mottelson B R 1975 *Nuclear Structure* vol 2 (New York: Benjamin)
[16] Bohr A and Mottelson B R 1969 *Nuclear Structure* vol 1 (New York: Benjamin)
[17] Nilsson S G 1955 *Mat. Fys. Medd. Dan. Vid. Selsk.* **N° 16** 29
[18] Bengtsson T and Ragnarsson I 1985 *Nucl. Phys.* A **436** 14
[19] Strutinsky V M 1968 *Nucl. Phys.* A **122** 1
[20] Ring P and Schuck P 1981 *The Nuclear Many-Body Problem* (Berlin: Springer)
[21] Veje E *et al* 1968 *Nucl. Phys.* A **109** 489
[22] McGowan F K and Milner W T 1981 *Phys. Rev.* C **23** 1926
[23] Shimizu Y R and Nakatsukasa T 1996 *Nucl. Phys.* A **611** 22